



The Impact of Interface Defect Density on the Performance of $\text{CH}_3\text{NH}_3\text{PbI}_3$ Based Solar Cell Using SCAPS-1D

Adamu Mohammed

Department of Physics, Kaduna State University, Kaduna PMB 2339, Kaduna, Nigeria
Author email: adamu.mohammed@kasu.edu.ng

Abstract

In this work, Solar Cell Capacitance Simulator-1D (SCAPS-1D) was utilized to study the interface defect densities with varying absorber layer thickness of perovskite solar cells. The planar heterojunction n-i-p structure was defined as $2\text{D-MoTe}_2/\text{CH}_3\text{NH}_3\text{PbI}_3/\text{Cu}_2\text{O}$, and its performance was simulated. Power conversion efficiency $> 23\%$ was realized at $< 10^{14} \text{ cm}^{-3}$ defect density at $2\text{D-MoTe}_2/\text{CH}_3\text{NH}_3\text{PbI}_3$ and $\text{CH}_3\text{NH}_3\text{PbI}_3/\text{Cu}_2\text{O}$ interfaces and $> 1.0 \mu\text{m}$ thickness of absorber layer. The study was carried out at 300K temperature. These results show constraints on numerical simulation for correlation between defect mechanism and performance.

Keywords: Perovskite solar cells, 2D-MoTe_2 , electron transport layer, interface defects, SCAPS-1D simulation, power conversion efficiency, fill factor, open-circuit voltage, short-circuit current density.

1. Introduction

Perovskite solar cells (PSCs) have garnered significant attention due to their remarkable power conversion efficiency (PCE) and potential for low-cost, scalable photovoltaic technology. The incorporation of two dimensional (2D) transition metal dichalcogenides (TMDCs), such as 2D-MoTe_2 as electron transport layers (ETLs) has emerged as a promising strategy to enhance PSC performance. However, interfacial defects between the 2D-MoTe_2 ETL and the $\text{CH}_3\text{NH}_3\text{PbI}_3$ (methylammonium lead iodide) perovskite absorber layer can significantly impact charge carrier dynamics, leading to recombination losses and reduced device efficiency.

PSCs have shown remarkable progress in recent years, with power conversion efficiencies (PCEs) exceeding 23% [1]. The planar heterojunction architecture, employing a perovskite absorber layer sandwiched between electron transport (ETL) and hole transport layers (HTL), has become a popular configuration[2].

2D TMDCs, such as MoTe_2 , have been explored as ETLs due to their, high electron mobility[3], Suitable energy band alignment [4, 5] and Enhanced stability [6]. Interface defects between the ETL and perovskite absorber layer can lead to, Increased recombination losses[7], reduced PCE[8] decreased V_{OC} and FF [9].

SCAPS-1D simulations have been employed to investigate the impact of interface defects on PSC performance [10], optimization of ETL thickness and material properties [11], the effects of doping concentration on the performance of PSC [12]

Perovskite solar cells are commonly synthesized by the method of one-step or two-step spin-on solution-based method [13]. Since the component materials are entirely different in their nature, defects are often found at the interfaces of this heterojunction device. These defects have significant effect on the performance of the cell [14].

While previous studies have investigated the impact of interface defects on PSC performance, the specific effects of defect density on 2D-MoTe₂ ETLs in CH₃NH₃PbI₃ solar cells remain unexplored.

This study investigates the impact of interface defect density on the performance of 2D- MoTe₂ ETLs and Cu₂O HTL in CH₃NH₃PbI₃ solar cells using SCAPS-1D simulations. Specifically, we examine the effects of interface defect density on key solar cell performance parameters: power conversion efficiency (PCE), open circuit voltage (V_{oc}), short circuit current density (J_{sc}) and fill factor (FF).

2. Method

The perovskite solar cell structure used in this work is shown in figure 1. Meanwhile the material properties of the design (n-i-p planer) is gotten from literature as indicated in table 1. Using these information, we constructed the basic structure 2D-MoTe₂/CH₃NH₃PbI₃/Cu₂O, where 2D-MoTe₂ serves as the electron transport layer, CH₃NH₃PbI₃ (methylammonium lead iodide) the light absorbing layer and Cu₂O the hole transport layer. Fluorine-doped Tin Oxide (FTO) is used as front contact and gold (Au) as back metal contact. The simulation was carried out at temperature (300 k) under Illumination of AM 1.5G (100 mW/cm²) or 1sun spectra, with V_{oc} highest limit of 1.8 V.

Table 1: Values representing the material properties used in the simulation.

Material property	Cu ₂ O[15]	CH ₃ NH ₃ PbI ₃ [16, 17]	2D-MoTe ₂ [17]
Thickness (um)	Varied	Varied	Varied
Band gap (eV)	2.17	1.50	1.01
Electron affinity (eV)	3.2	3.90	3.91
Dielectric permittivity	7.5	6.50	7.20
CB effective density of states (cm ⁻³)	2.0x10 ¹⁸	2.2x10 ¹⁸	1.8x10 ¹⁹
VB effective density of states (cm ⁻³)	1.8x10 ¹⁸	2.2x10 ¹⁸	1.8x10 ¹⁹
Electron mobility (cm ² /V.s)	20	20	1.6x10 ⁴
Hole mobility (cm ² /V. s)	80	20	2.1x10
Shallow Acceptor density NA (cm ⁻³)	varied	1.0x10 ¹⁵	0.0
Shallow donor density ND (cm ⁻³)	1x10 ¹⁴	0.0	1.0x10 ¹⁵

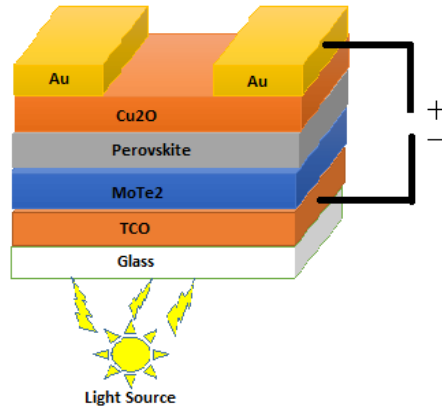


Figure 1: Schematic structure of the simulated PSC

SCAPS-1D version 3.3.10, a software developed at the Department of Electronics and Information Systems (ELIS) of the University of Ghent, Belgium was employed for the simulation [18, 19]. The software works one of the best among its kind [20], it works based on Poisson's equation and the continuity equation of both charge carriers[21], these equations are given as

$$\nabla^2 \varphi = \frac{q}{\varepsilon} (n - p + N_A - N_D) \quad 1$$

Where, N_A is the acceptor concentration, N_D is the donor concentration and φ is the electrostatic potential, q electric charge and the ε dielectric permittivity of the semiconductor.

$$\nabla J_n - q \frac{\partial n}{\partial r} = +qR \quad 2$$

$$\nabla J_p + q \frac{\partial p}{\partial r} = -qR \quad 3$$

Here, J_n represents the current density for electrons, J_p represents the current density for holes and R is the rate of carrier recombination

$$J_n = qn\mu_n E + qD_n \nabla n \quad 4$$

$$J_p = qp\mu_p E - qD_p \nabla p \quad 5$$

Where, D_p is the diffusion coefficient for holes and D_n is the diffusion coefficient for electrons. The code iterates the equations using Newton Raphson and Gunmel iteration method [22] to produce the results

After optimizing the performance parameters, we then vary the interface defect density in the range of 10^{10} to 10^{18} cm^{-2} to cover the low 10^{12} and high 10^{16} cm^{-2} defect densities as given by [16] at the 2D-MoTe₂/CH₃NH₃PbI₃ and CH₃NH₃PbI₃/Cu₂O interfaces with the corresponding CH₃NH₃PbI₃ thickness respectively and find out the effect on the cell performance parameters (PCE, Voc, Jsc and FF).

3. Results and Discussion

The SCAPS simulations were performed based on parameters obtained from different experimental and theoretical research papers. Each component of the perovskite solar cell has a significant influence on the device's performance. After designing the cell FTO/2D-MoTe₂/CH₃NH₃PbI₃/Cu₂O/Au keeping all the parameters the same. we optimized the performance parameters, the result of the optimized cell is given in table 2. The cell gives an optimum power conversion efficiency of 24%.

Optimization of the electron transport layer is also very much important to achieve higher photovoltaic performance in perovskite solar cells. The ETL is responsible for extracting and transporting the photogenerated electrons. Optimization of ETL can control the charge recombination rates in perovskite solar cells. Fig. 3b represents the plots of performance parameters as a function of ETL thickness that is varied in the range of 10–100 nm. It was observed very insignificant decreases in open-circuit voltage as the layer thickness increases, then it becomes constant followed by a slight decrease which may be due to the increase in the series resistance and recombination in the device. The highest obtained VOC is at 10 nm with a value of ~1.09V. The short circuit current density(JSC) first goes through a small decrease as we increase the thickness, then the JSC decreases almost following a linear curve, getting a minimum value at 100 nm of ETL thickness. The fill factor (FF) and efficiency curves display a similar nature. Both of them increase as the thickness is varied in the range of 10 nm–40 nm. On further increasing the thickness, the FF and PCE become almost constant with a negligible variation. So, for the optimum device configuration, the ETL thickness should be in the range of 40 nm–60 nm which is nearly equal to carrier diffusion length.

It is observed that the device with Cu₂O shows better performance as compared to others. The performance parameters obtained after simulation with different HTLs are s

Table 2: Optimized performance parameters of the device.

Performance parameters	
Open circuit voltage (Voc)	1.1264 V
Short circuit current density (Jsc)	24.450764 mA/cm ²
Fill factor (FF)	86.34 %
Power Conversion Efficiency (PCE)	23.78 %

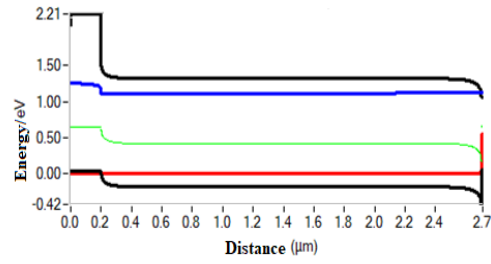


Figure 2: Band Diagram

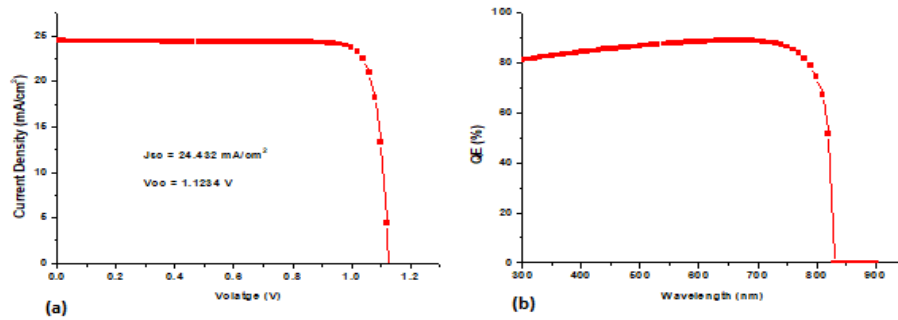


Figure 3: (a) The IV characteristics (b) Quantum Efficiency of the PSC

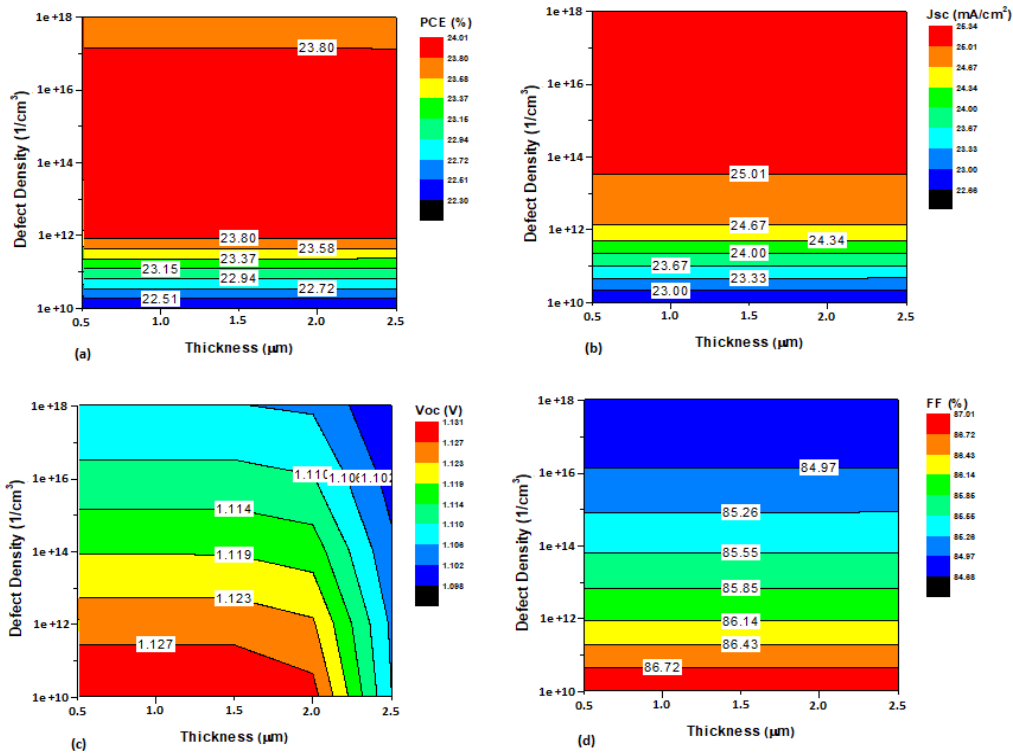


Figure 4: Contour graphs of $\text{CH}_3\text{NH}_3\text{PbI}_3$ solar cell performance parameters dependency on of interface defect density at 2D-MoTe₂/ $\text{CH}_3\text{NH}_3\text{PbI}_3$ interface and $\text{CH}_3\text{NH}_3\text{PbI}_3$ thickness.

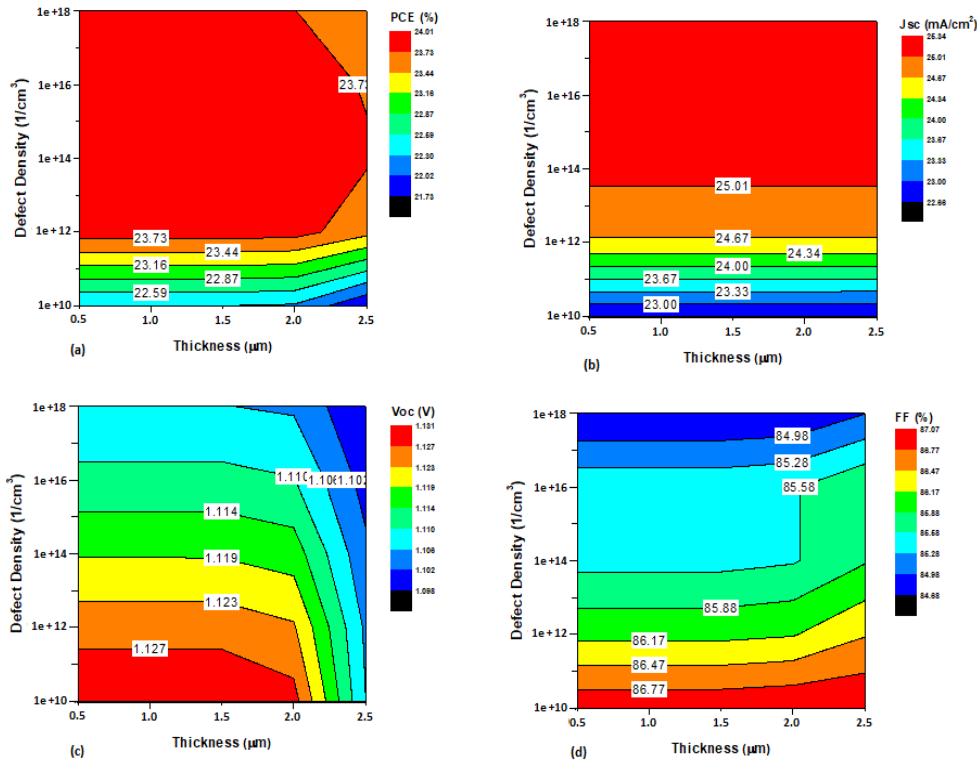


Figure 5: Contour graphs of $\text{CH}_3\text{NH}_3\text{PbI}_3$ solar cell performance parameters dependency on of interface defect density at Cu₂O/ $\text{CH}_3\text{NH}_3\text{PbI}_3$ interface and $\text{CH}_3\text{NH}_3\text{PbI}_3$ thickness.

Conclusion

This study optimized perovskite solar cell with a n-i-p configuration using SCAPS-1D simulator. 2D-MoTe₂/CH₃NH₃PbI₃/Cu₂O configuration was the primary modelled solar cell. Based on the simulation result, the PCE > 23% was obtained with V_{oc} of 1.2 V, FF 86%, and J_{sc} > 24 mA/cm². Increase in absorber layer thickness caused the perovskite solar cell efficiency to rapidly increase. Suitable absorber thickness > 1.0 μm and interfaces defect density of < 10¹⁴ cm⁻³ were found to be optimal for ETL and HTL/CH₃NH₃PbI₃. In the second part, we obtained the CdS/absorber layer thickness. We changed the absorber layer thickness (0.5–2.0 μm) and tuned the defect density (10¹⁰–10¹⁸ cm⁻³).

A similar trend was observed although the device performance was more sensitive to the defect density. We discovered that the defect density has significant effect on perovskite solar cells, and increasing the thickness of absorber layer up to the certain point can overcome this issue. This work could provide important information for optimization of perovskite solar cells

Declaration of Competing Interest

The author declare that they have no known competing financial interests or personal relationships that could have appeared to influence the work reported in this paper.

Acknowledgement

We thank the Department of Electronics and Information Systems (ELIS) of the University of Ghent, Belgium for providing the software for free, we also acknowledged the help offered by Physics Department Kaduna State University, Kaduna Nigeria, for providing the essential computing systems.

References:

- [1] G. Yan, Y. Yuan, M. Kaba, and T. Kirchartz, "Visualizing Performances Losses of Perovskite Solar Cells and Modules: From Laboratory to Industrial Scales," *Advanced Energy Materials*, vol. 15, no. 3, p. 2403706, 2025.
- [2] J.-F. Liao, W.-Q. Wu, Y. Jiang, J.-X. Zhong, L. Wang, and D.-B. Kuang, "Understanding of carrier dynamics, heterojunction merits and device physics: towards designing efficient carrier transport layer-free perovskite solar cells," *Chemical Society Reviews*, vol. 49, no. 2, pp. 354-381, 2020.
- [3] Z. Zhou, J. Lv, C. Tan, L. Yang, and Z. Wang, "Emerging Frontiers of 2D Transition Metal Dichalcogenides in Photovoltaics Solar Cell," *Advanced Functional Materials*, p. 2316175, 2024.
- [4] Y. Wang, S. Ji, and B. Shin, "Interface engineering of antimony selenide solar cells: A review on the optimization of energy band alignments," *Journal of Physics: Energy*, vol. 4, no. 4, p. 044002, 2022.
- [5] S. Farhan, A. H. Raza, L. Li, S. Yang, and Y. Wu, "Designed 2D/2D F-doped TiO₂@ ZnIn₂S₄ heterojunction for efficient photo-utilization hydrogen generation," *Journal of Colloid and Interface Science*, vol. 681, pp. 1-15, 2025.
- [6] J. Suo, B. Yang, D. Bogachuk, G. Boschloo, and A. Hagfeldt, "The dual use of SAM molecules for efficient and stable perovskite solar cells," *Advanced Energy Materials*, vol. 15, no. 2, p. 2400205, 2025.
- [7] M. M. Haque *et al.*, "Study on the interface defects of eco-friendly perovskite solar cells," *Solar Energy*, vol. 247, pp. 96-108, 2022.
- [8] J. D. Culpepper, M. M. Scherer, T. C. Robinson, A. Neumann, D. Cwiertny, and D. E. Latta, "Reduction of PCE and TCE by magnetite revisited," *Environmental Science: Processes & Impacts*, vol. 20, no. 10, pp. 1340-1349, 2018.
- [9] J. Y. Ye, T. Reindl, A. G. Aberle, and T. M. Walsh, "Performance degradation of various PV module technologies in tropical Singapore," *IEEE Journal of Photovoltaics*, vol. 4, no. 5, pp. 1288-1294, 2014.
- [10] M. Aliaghaee, "Optimization of the perovskite solar cell design with layer thickness engineering for improving the photovoltaic response using SCAPS-1D," *Journal of Electronic Materials*, vol. 52, no. 4, pp. 2475-2491, 2023.
- [11] I. Gulomova, O. Accouche, R. Aliev, Z. Al Barakeh, and V. Abduazimov, "Optimizing Geometry and ETL Materials for High-Performance Inverted Perovskite Solar Cells by TCAD Simulation," *Nanomaterials*, vol. 14, no. 15, p. 1301, 2024.
- [12] S. T. Jan and M. Noman, "Influence of layer thickness, defect density, doping concentration, interface defects, work function, working temperature and reflecting coating on lead-free perovskite solar cell," *Solar Energy*, vol. 237, pp. 29-43, 2022.
- [13] J. R. M. Bojorquez, "Efficient Light Harvesting for Photovoltaics Using Multifunctional Quantum Dot Arrays," The University of Texas at San Antonio, 2024.

- [14] J. Zhu, D. Zhou, R. Lu, X. Liu, and D. Wan, "C2DEM-YOLO: improved YOLOv8 for defect detection of photovoltaic cell modules in electroluminescence image," *Nondestructive Testing and Evaluation*, vol. 40, no. 1, pp. 309-331, 2025.
- [15] A. K. Singh, S. Srivastava, A. Mahapatra, J. K. Baral, and B. Pradhan, "Performance optimization of lead free-MASnI₃ based solar cell with 27% efficiency by numerical simulation," *Optical Materials*, vol. 117, p. 111193, 2021.
- [16] M. Chowdhury *et al.*, "Effect of deep-level defect density of the absorber layer and n/i interface in perovskite solar cells by SCAPS-1D," *Results in Physics*, vol. 16, p. 102839, 2020.
- [17] M. Adamu, S. Alhassan, S. G. Abdu, and M. M. Aliyu, "Ultra-Thin 2D MoTe₂ for Electron Transport Material Application in Perovskite Solar Cell: A Theoretical Approach," *Physics Access*, vol. 4, no. 1, pp. 32-43, 2024.
- [18] A. C. Ozurumba *et al.*, "SCAPS-1D simulated organometallic halide perovskites: A comparison of performance under Sub-Saharan temperature condition," *Heliyon*, vol. 10, no. 8, 2024.
- [19] M. F. H. Haque and M. L. Rahman, "Design and development of CsSnI₃ solar cell using SCAPS-1D simulation," Brac University, 2024.
- [20] E. Danladi, M. Kashif, A. Ichoja, and B. B. Ayiye, "Modeling of a Sn-based HTM-free perovskite solar cell using a one-dimensional solar cell capacitance simulator tool," *Transactions of Tianjin University*, vol. 29, no. 1, pp. 62-72, 2023.
- [21] W. Zulhafizhazuan, K. Sobayel, S. Shafian, S. Sepeai, and M. A. Ibrahim, "Preliminary study on planar-mixed dimensional Cs₃Bi₂I₉ solar cells: SCAPS-1D simulation and experimental analysis," *Interactions*, vol. 246, no. 1, p. 29, 2025.
- [22] S. Mann, E. Fadel, S. S. Schoenholz, E. D. Cubuk, S. G. Johnson, and G. Romano, " ∂ PV: An end-to-end differentiable solar-cell simulator," *Computer Physics Communications*, vol. 272, p. 108232, 2022.